Supporting Information

Exchange Coupled Co(II) Based Layered and Porous Metal Organic Frameworks: Structural Diversity, Gas Adsorptions and Magnetic Properties

Ajit Kumar Kharwar, Sanjit Konar *

Department of Chemistry, Indian Institute of Science Education and Research, (IISER), Bhopal By-pass Road, Bhauri, Bhopal-462066, India. E-mail: skonar@iiserb.ac.in

Crystallographic Analysis of the Disorder

Complex 3: The disorder in this structure is challenging to model. Not only are the camphoric ligands disordered over two 'end-over' rotations, but the methyl group within each main disorder is then disordered over two sites, too. The methyl groups in this secondary disorder have been kept in the same PART for simplicity and spurious hydrogen atom interactions may be detected by CheckCif. However, these distances are NOT included in the CIF files as bonds.

The main disorder in one group is 70/30 while it is 60/40 in the other ligand. The minor disorder has been set to 1/2 in both cases.

A strong overall RIGU restraint has been used for all non-H atoms to keep the ADPs reasonable. Alternatively, an isotropic refinement could have been chosen, but the RIGU approach allows for easier evaluation of the presented model.

The structure is based on relatively weak data (mean I/sigma ~ 8). No overall atomic naming scheme has been introduced, but ligating N and O atoms have been named sensibly.

A solvent mask has been used to mask the presence of 4 molecules of MeCN per asymmetric unit. Olex2.mask was used and its use has been reported properly in the CIF file.

Complex 4: There is complicated disorder present here, where the end of the ligand containing the O-Me group is disordered over two positions. This disorder is 'concealed' by symmetry -- i.e. both disordered parts are the same entity. Intermingled with this are also an estimated two disordered MeCN solvent molecules which cannot be sensibly modelled well (we tried), giving rise to residual density peaks in this part. Given the complexity of the model, this appears to be the sensible thing to do.

A solvent mask has also been used, identifying a further molecule of MeCN in the masked area.

The masked, as well as the estimated molecules of solvation, have been included in the formula unit and all follow-on quantities.

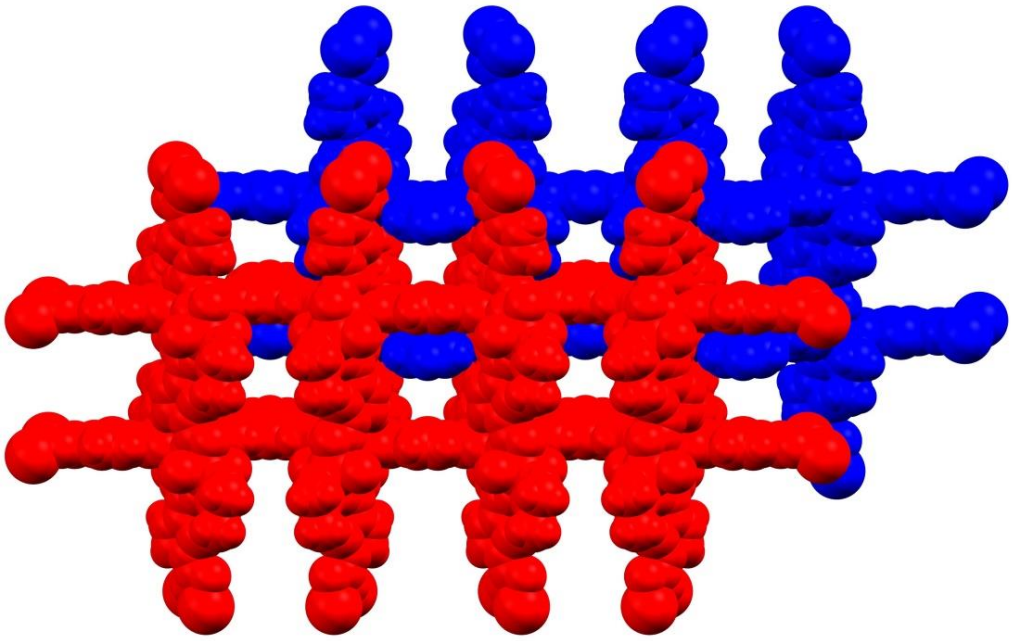

Fig. S1 Space-fill representation of 2D layered structure of **1** showing 1D pore along *c* axis.

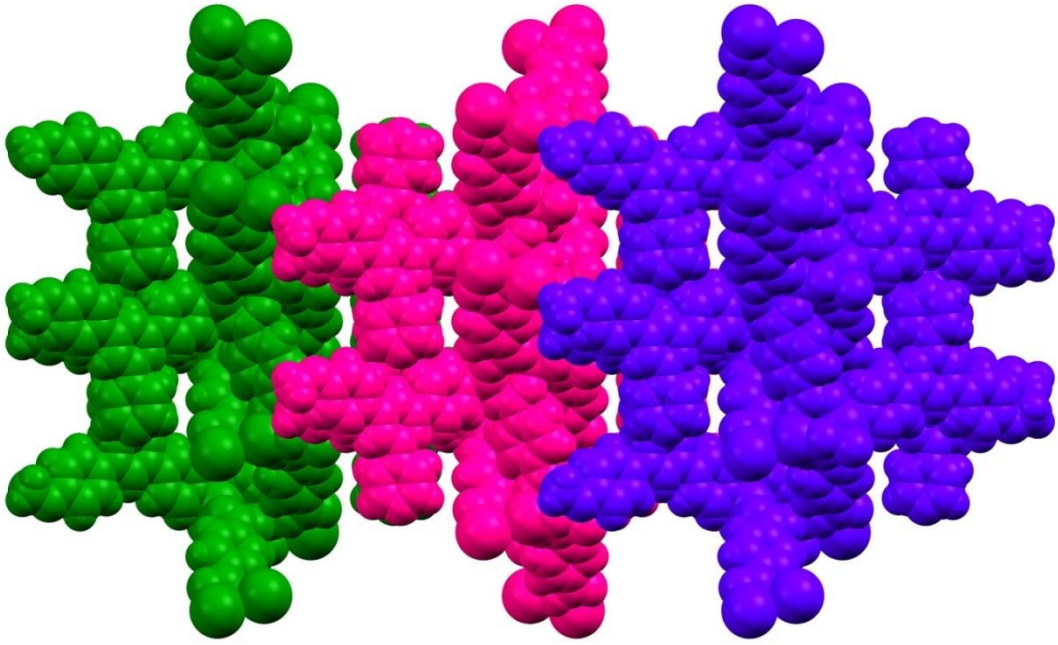

Fig. S2 2D layered structure of **2** (space-fill representation along *c* axis).

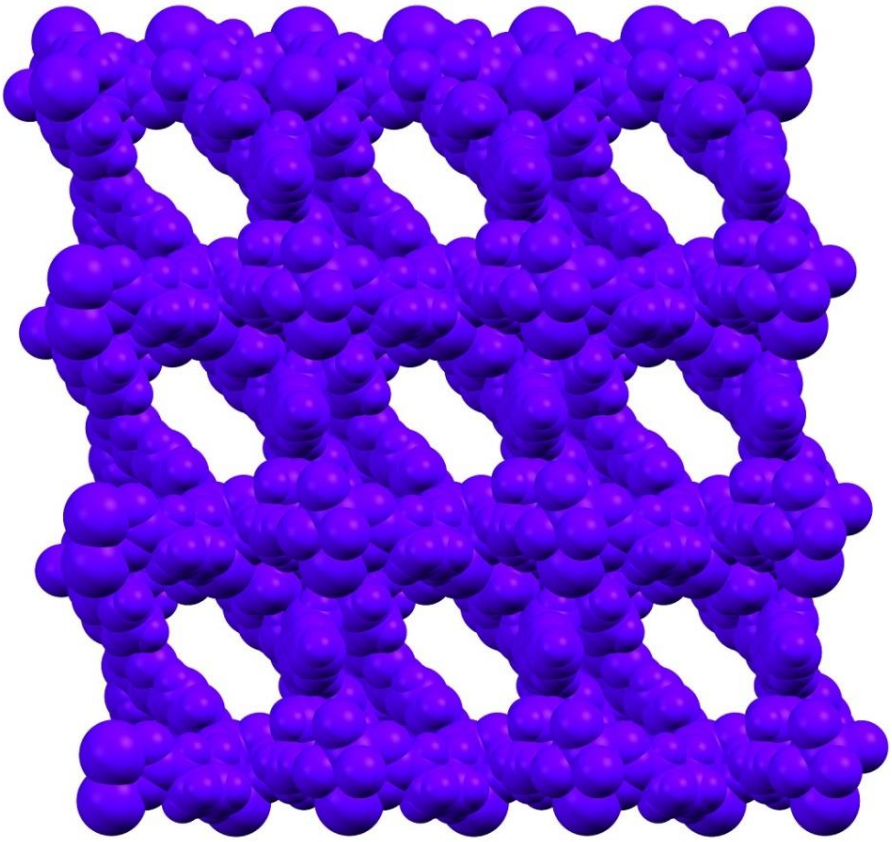

Fig. S3 3D space-fill packing of **3** showing 1D pore along *a* axis.

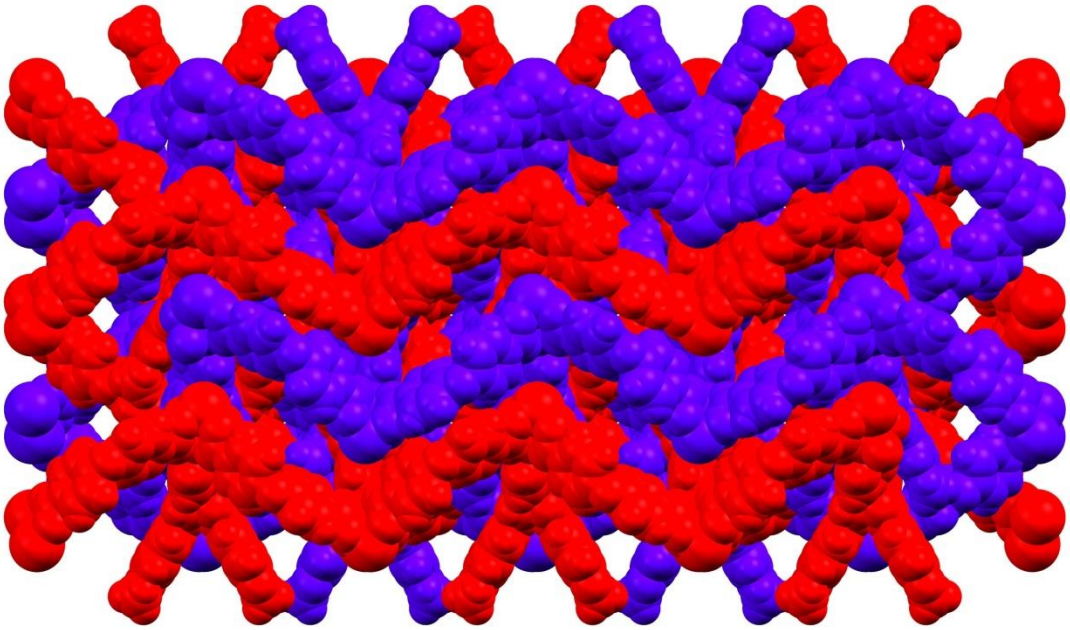

Fig. S4 3D space-fill packing MOF **4** showing 2-fold interpenetrated structure along *c* axis.

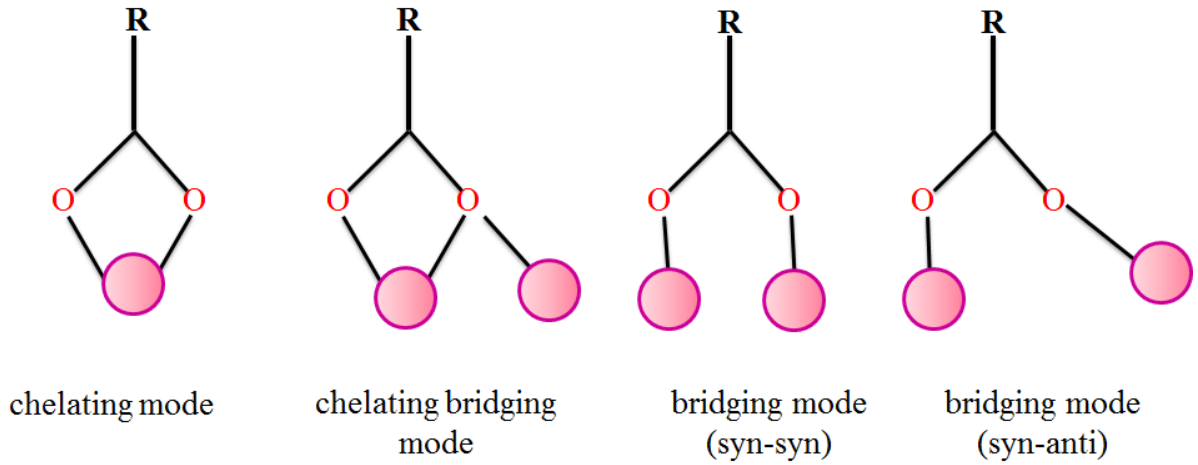

Fig. S5 Binding mode of different carboxylate in **1**-**4**.

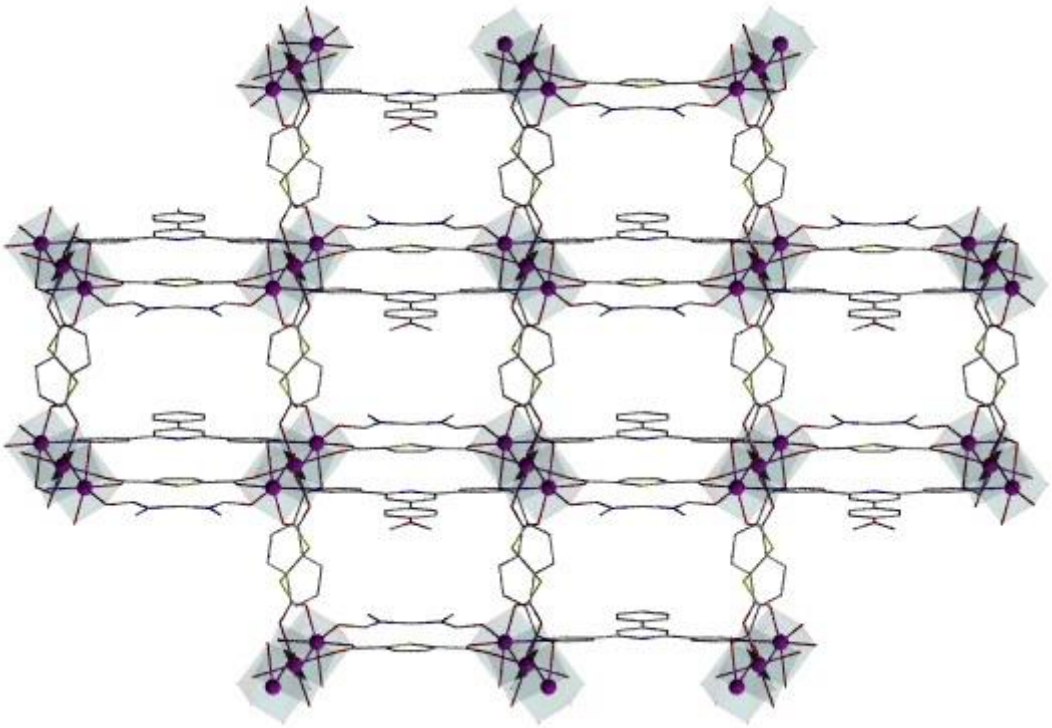

Fig. S6 Rectangular 2D sheet of **1**.

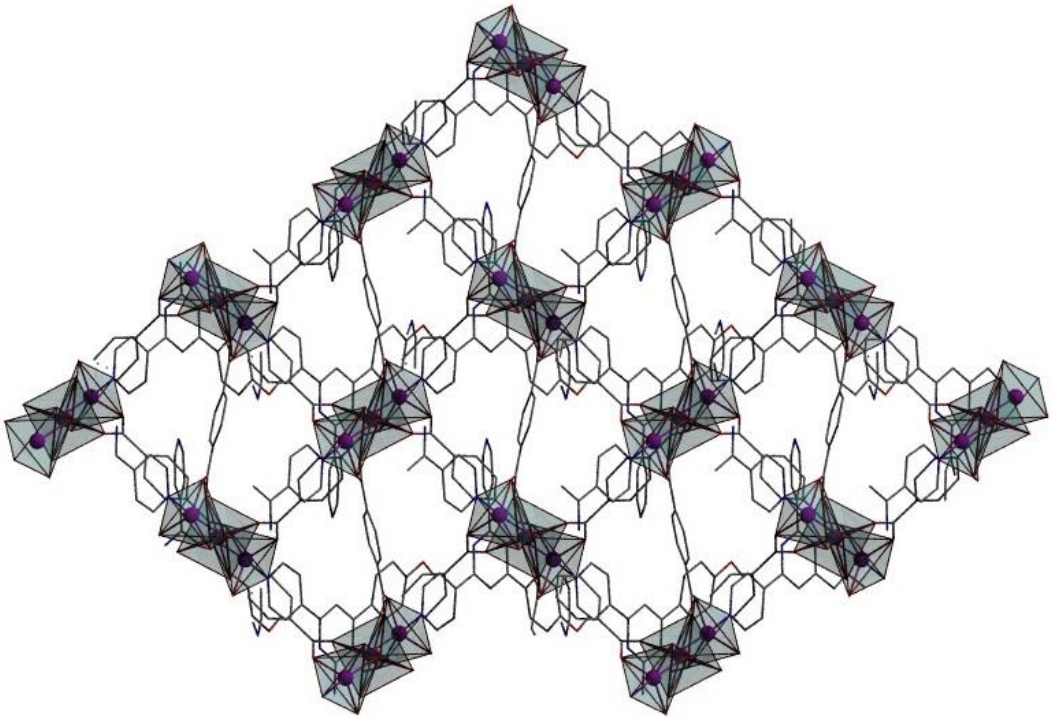

Fig. S7 Triangular 2D sheet of **2**.

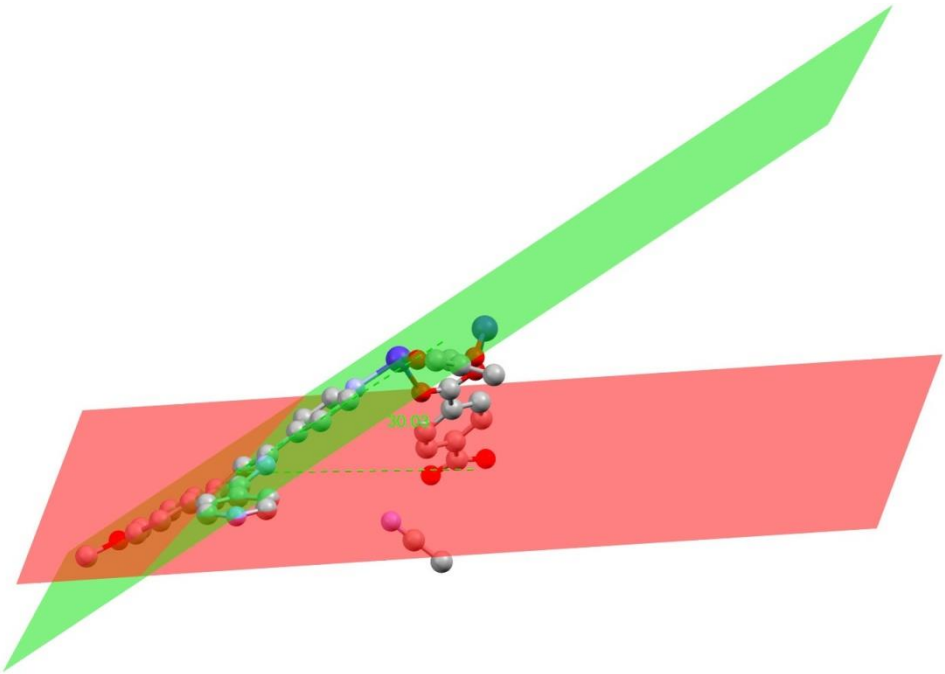

Fig. S8 Dihedral angle (30.03) between the two planes of aromatic rings of neutral ligand in **2**.

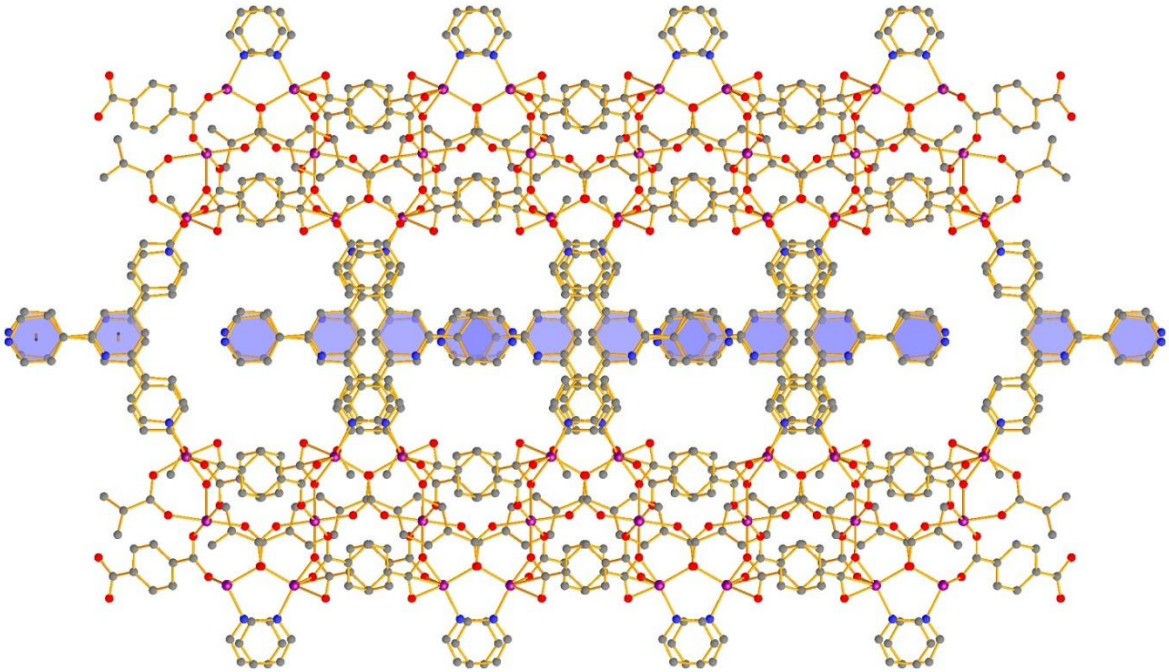

Fig. S9. π–π stacking in **2** along *c* axis.

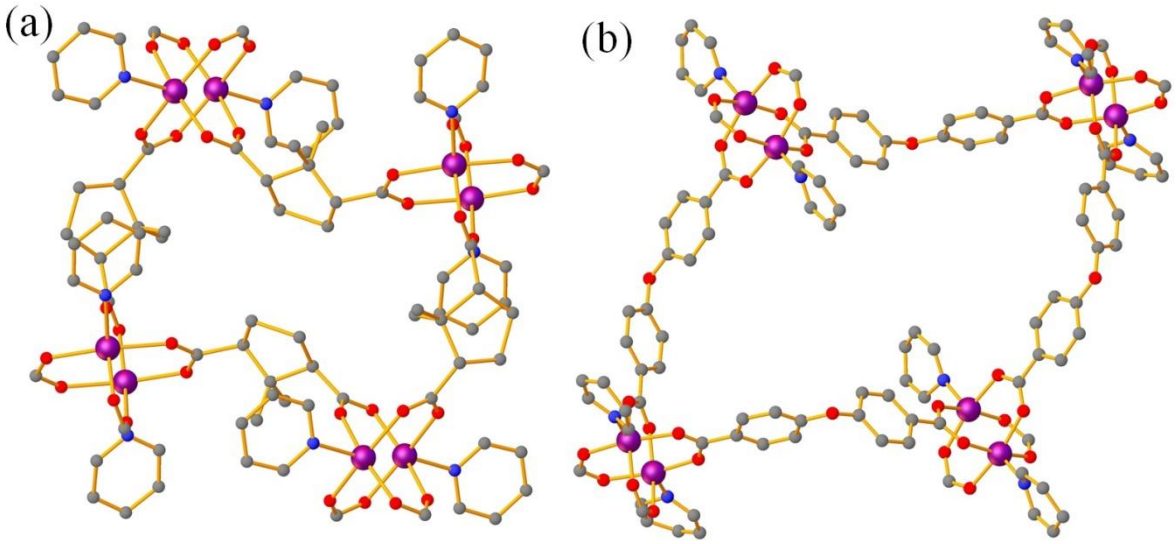

Fig.S10 (a) [4+4] metallacycle of MOF **3** and (b) MOF **4**.

Shape Measurement

Table S1

ML6 (Possible Structures)			ML5 (Possible Structures)		
HP-6	1 D6h	Hexagon	PP-5	1 D5h	Pentagon
PPY-6	2 C5v	Pentagonal pyramid	vOC-5	2 C4v	Vacant octahedron
OC-6	3 Oh	Octahedron	TBPY-5	3 D3h	Trigonal bipyramid
TPR-6	4 D3h	Trigonal prism	SPY-5	4 C4v	Spherical square pyramid
JPPY-6	5 C5v	Johnson pentagonal pyramid J2	JTBPY-5	5 D3h	Johnson trigonal bipyramid J12

MOF 1

Structure [ML6]	HP-6	PPY-6	**OC-6**	TPR-6	JPPY-6
Co1	29.392	22.493	**2.035**	13.472	26.342
Co2	29.257	28.238	**0.254**	16.137	31.319
Co3	29.392	22.439	**2.035**	13.472	26.342

MOF 2

Structure [ML5]	PP-5	vOC-5	TBPY-5	**SPY-5**	JTBPY-5
Co1	27.473	3.758	4.132	**2.485**	6.057
Co3	27.473	3.758	4.132	**2.485**	6.057

Structure [ML6]	HP-6	PPY-6	**OC-6**	TPR-6	JPPY-6
Co2	31.751	29.525	**0.081**	16.122	32.883

MOF 3

Structure [ML5]	PP-5	vOC-5	TBPY-5	**SPY-5**	JTBPY-5
Co1	30.408	0.868	5.878	**0.674**	8.141
Co2	30.408	0.868	5.878	**0.674**	8.141

MOF 4

Structure [ML6]	PP-5	vOC-5	TBPY-5	**SPY-5**	JTBPY-5
Co1	30.692	0.452	6.030	**0.574**	8.053
Co2	30.692	0.452	6.030	**0.574**	8.053

Highlighted red colour shows the actual geometries of the metal centres with minimum distortions.

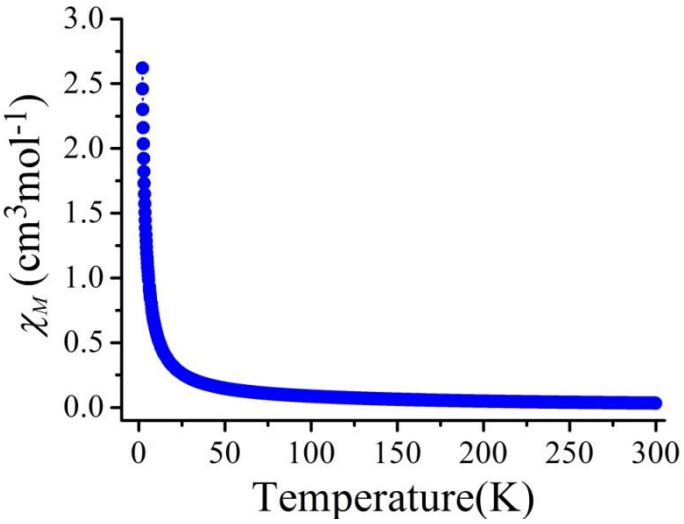

Fig. S11 Thermal dependence of molar magnetic moment of **1**.

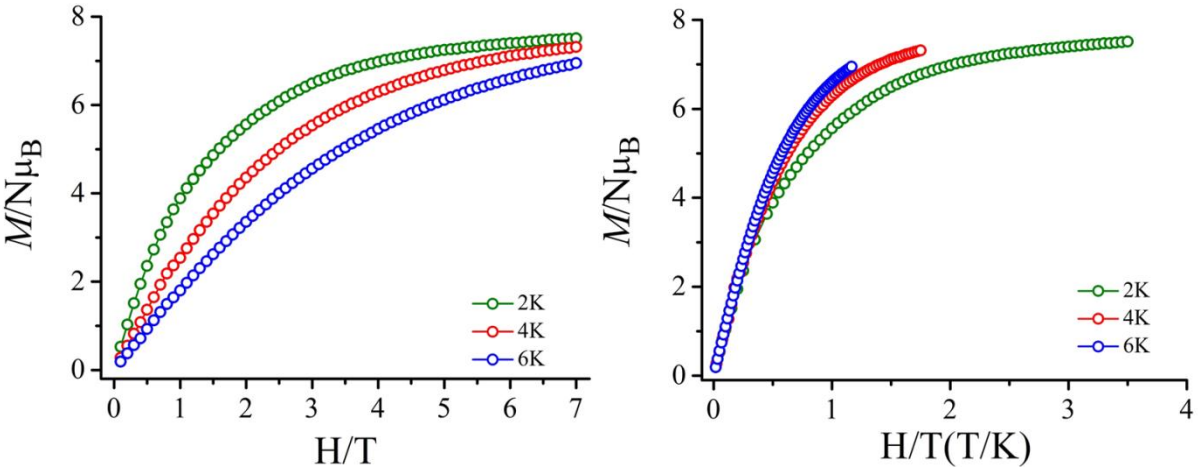

Fig. S12 M/N$_{\mu B}$ *vs.* H plot for complex **1** (left side) at the indicated temperatures, and reduced magnetization plot (right side).

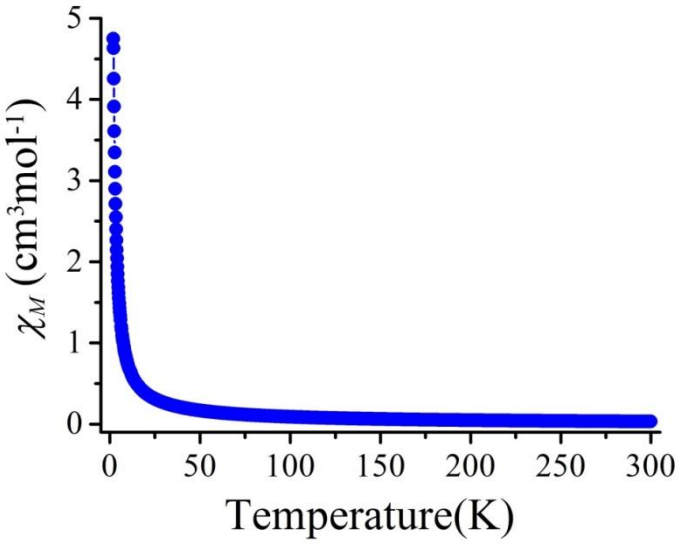

Fig. S13 Thermal dependence of molar magnetic moment of MOF **2**.

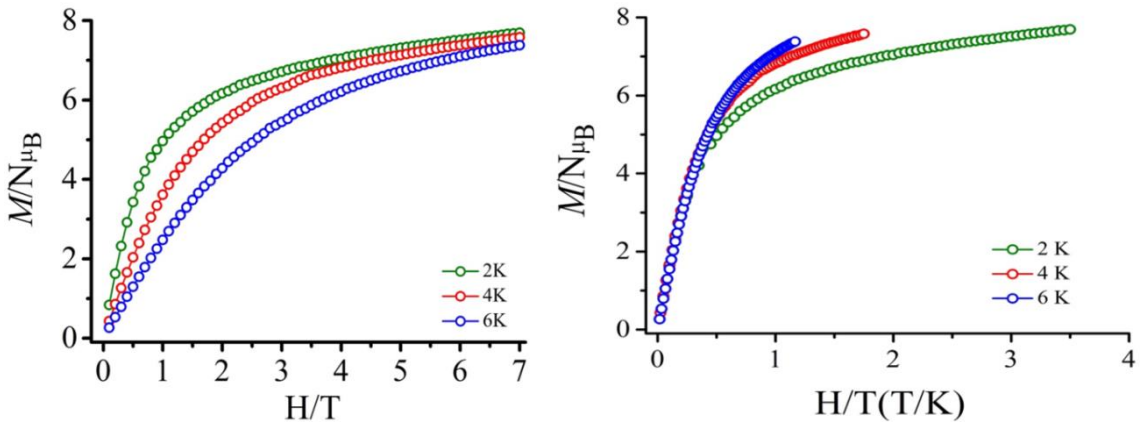

Fig. S14 $M/N_{\mu B}$ *vs.* H plot for complex **2** (left side) at the indicated temperatures, and reduced magnetization plot (right side).

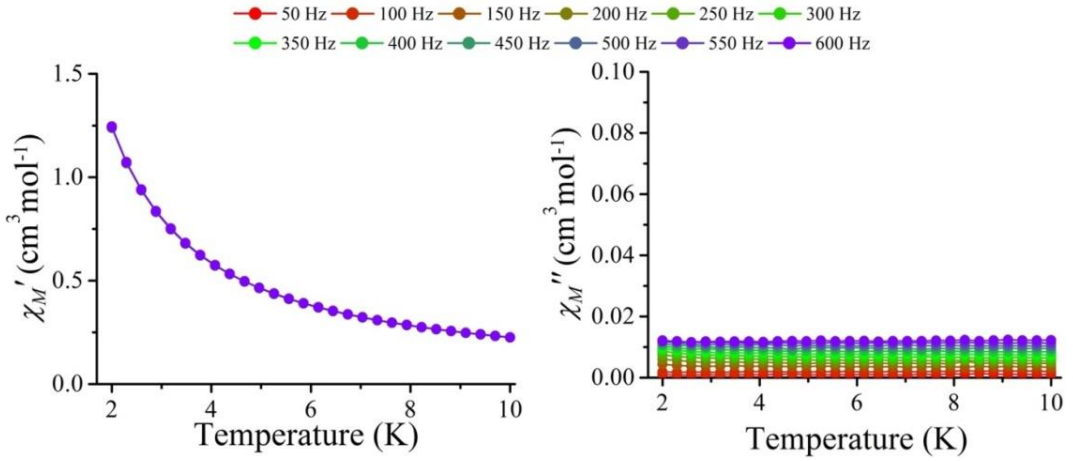

Fig. S15 Frequency dependence of the in-phase (χ') and out-of-phase (χ'') ac susceptibilities measured under zero dc field for **2**.

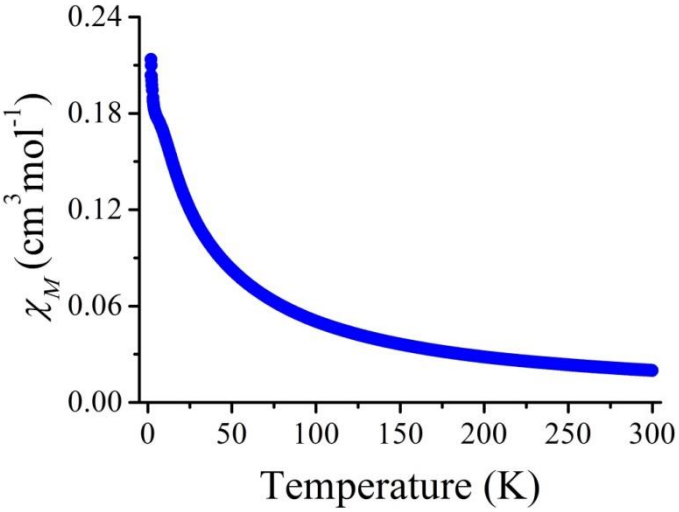

Fig. S16 Thermal dependence of molar magnetic moment of MOF **3**.

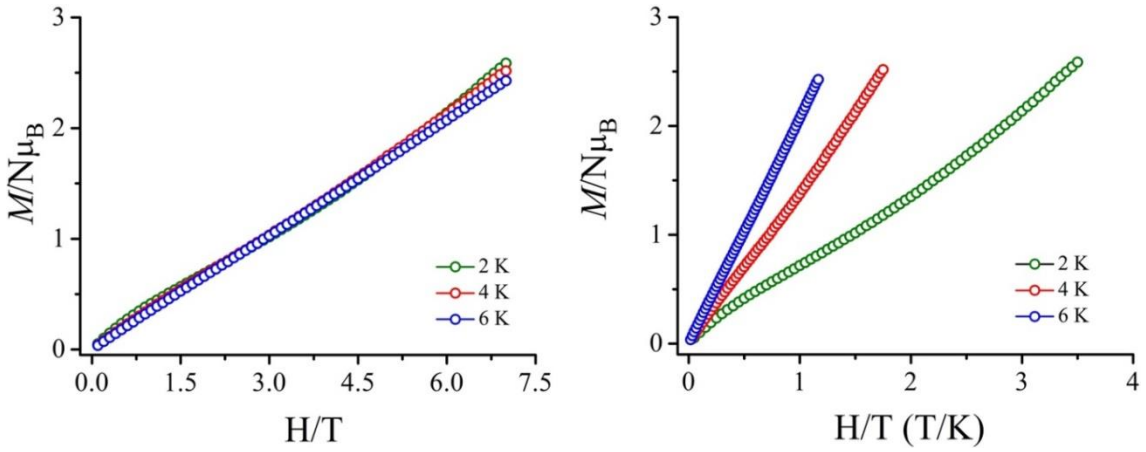

Fig. S17 $M/N_{\mu B}$ *vs.* H plot for complex **3** (left side) at the indicated temperatures, and reduced magnetization plot (right side).

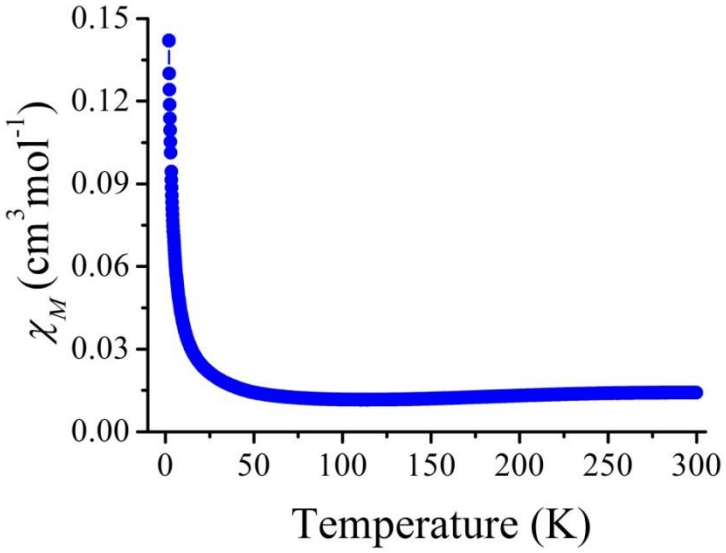

Fig. S18 Thermal dependence of molar magnetic moment of MOF **4**.

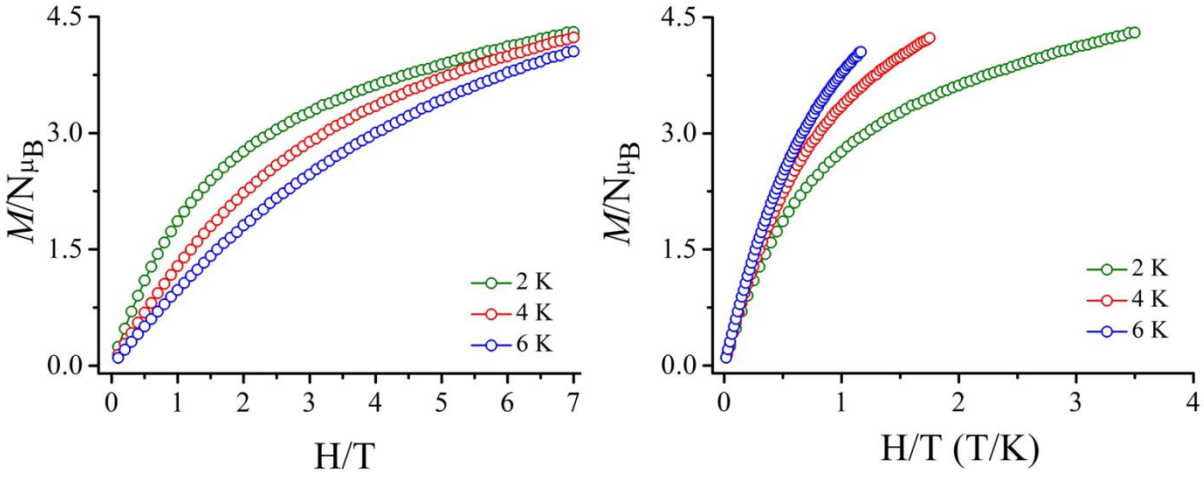

Fig. S19 $M/N_{\mu B}$ *vs.* H plot for complex **4** (left side) at the indicated temperatures, and reduced magnetization plot (right side).

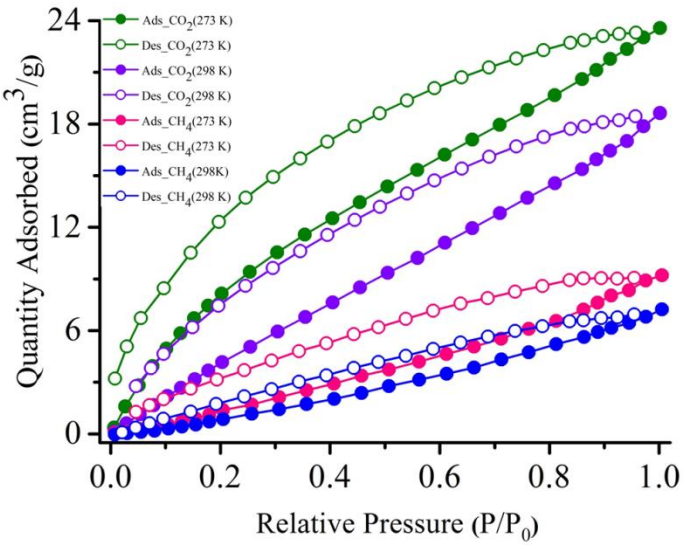

Fig. S20 Adsorption isotherms of CO_2/CH_4 for **2** at around room temperature (273 K and 298 K) and 1 atm.

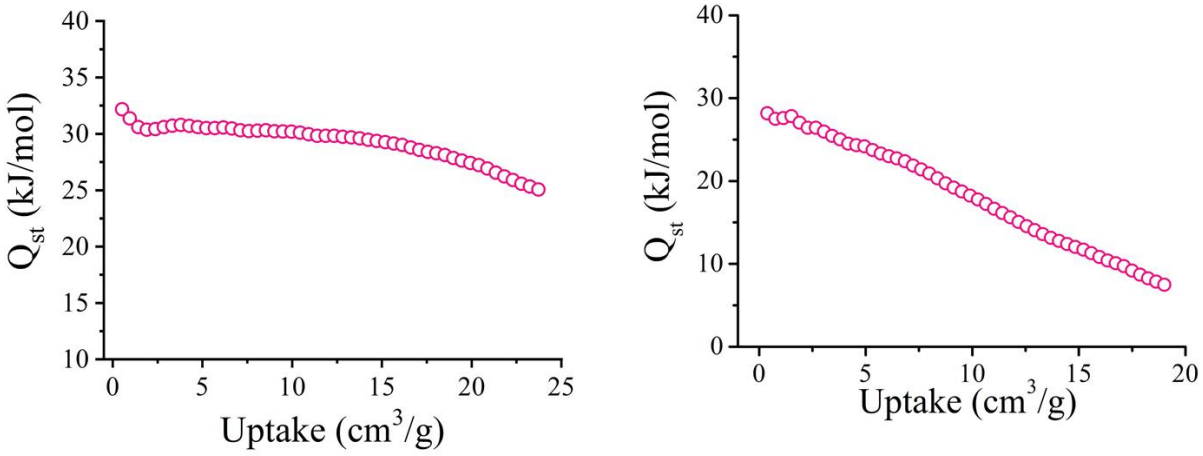

Fig. S21 Isosteric heat plots with low CO_2 loading of **1** (left side) and **2** (right side).

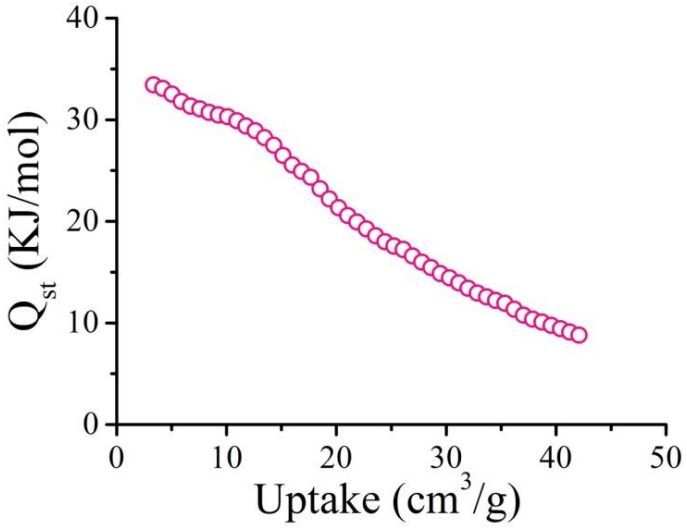

Fig. S22 Isosteric heat plot with low CO_2 loading of **3**.

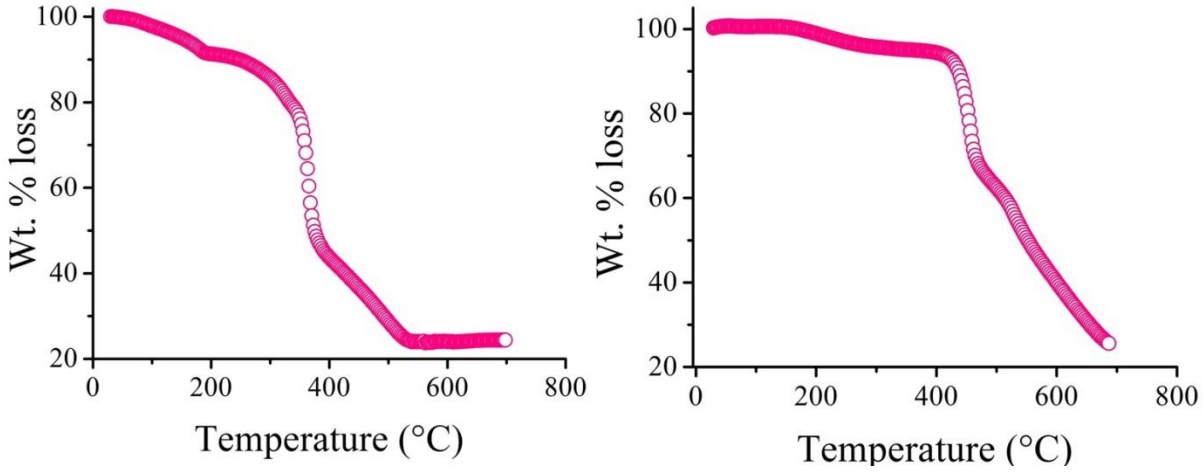

Fig. S23 TGA data of **1** (left side) and **2** (right side).

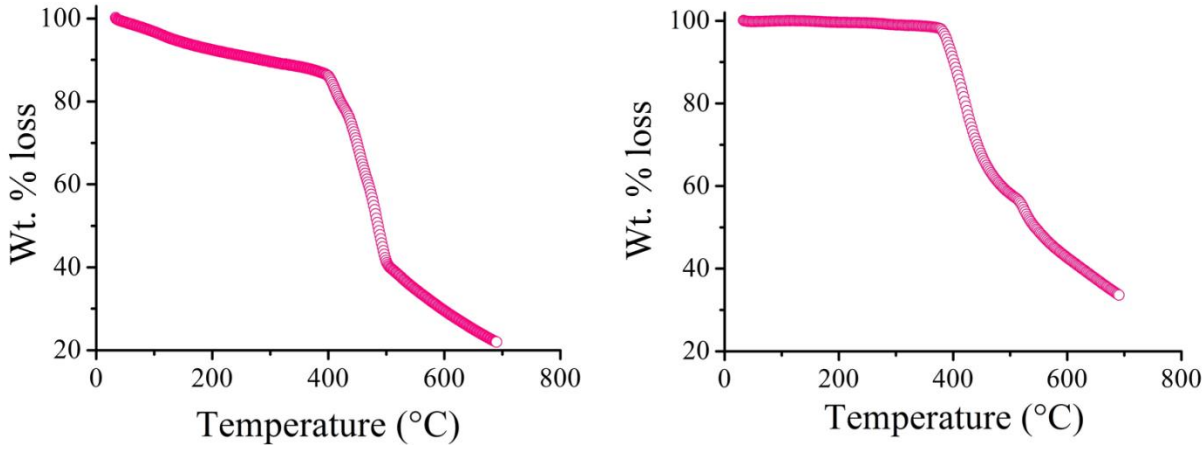

Fig. S24 TGA data of **3** (left side) and **4** (right side).

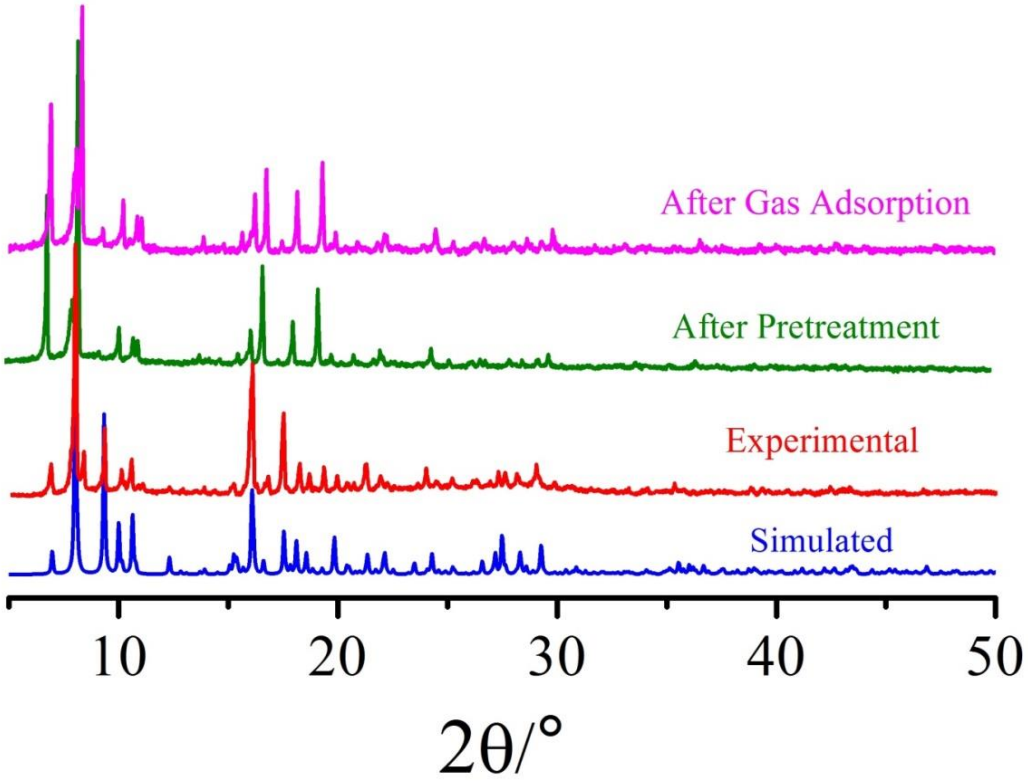

Fig. S25 PXRD pattern of MOF **1**.

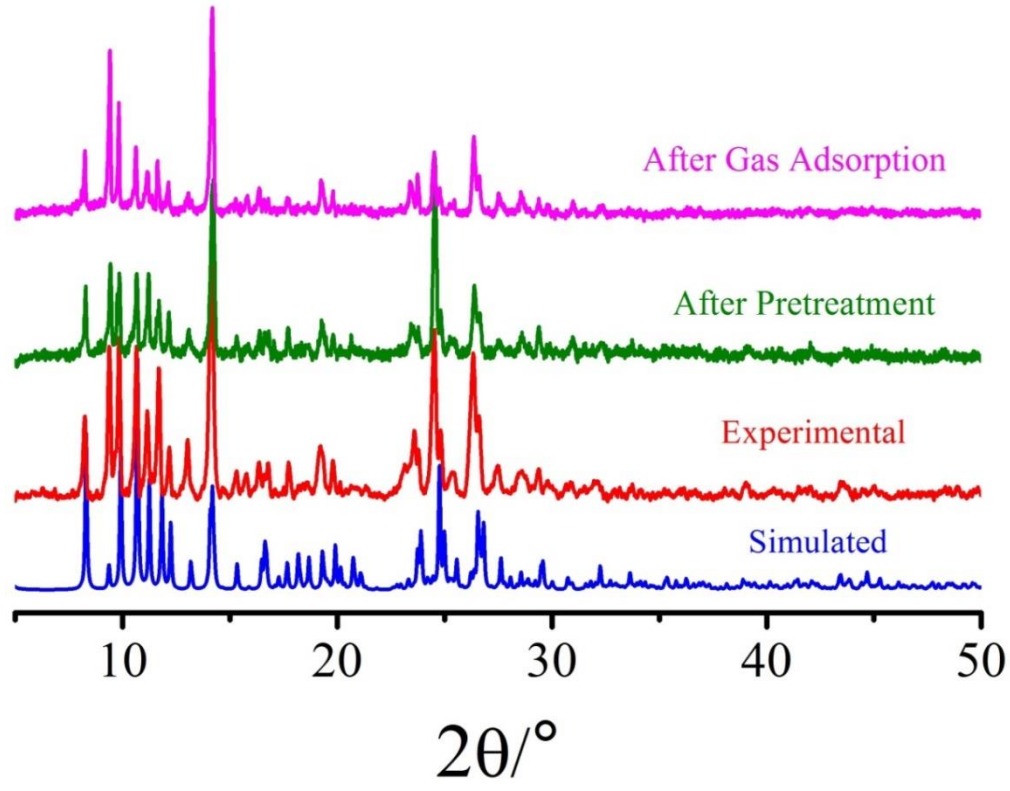

Fig. S26 PXRD pattern of MOF **2**.

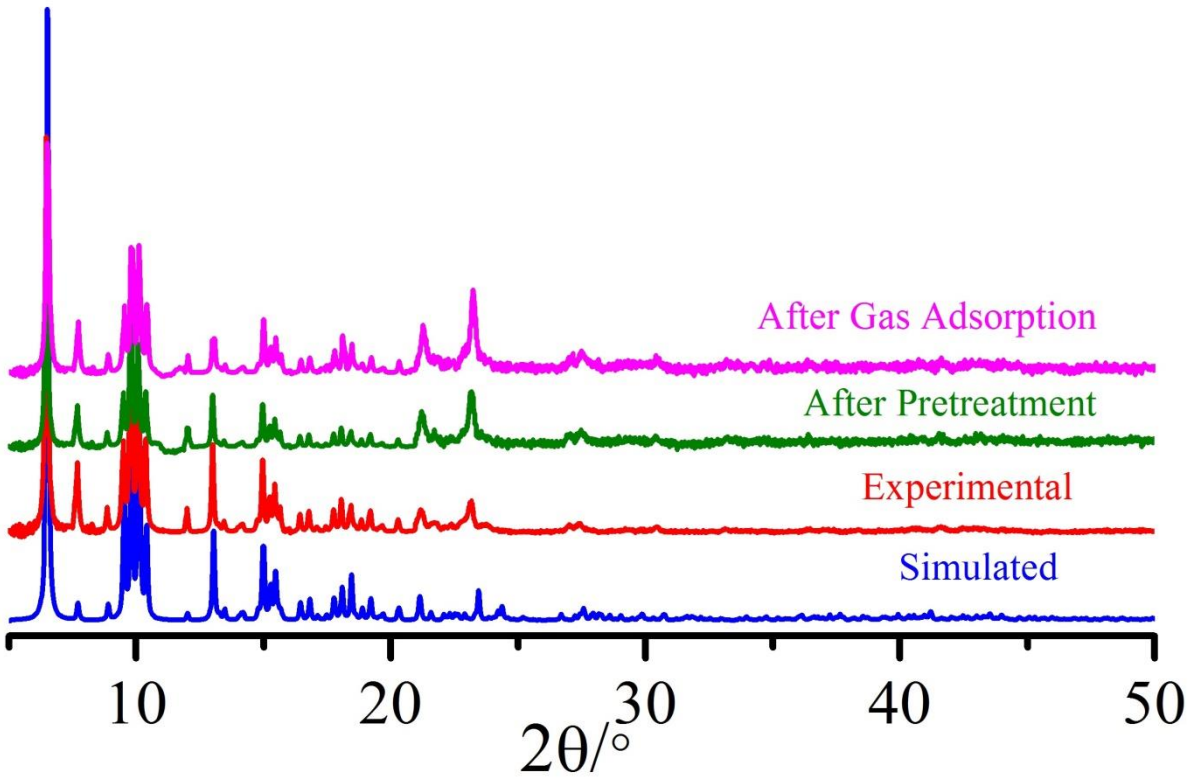

Fig. S27 PXRD pattern of MOF **3**.

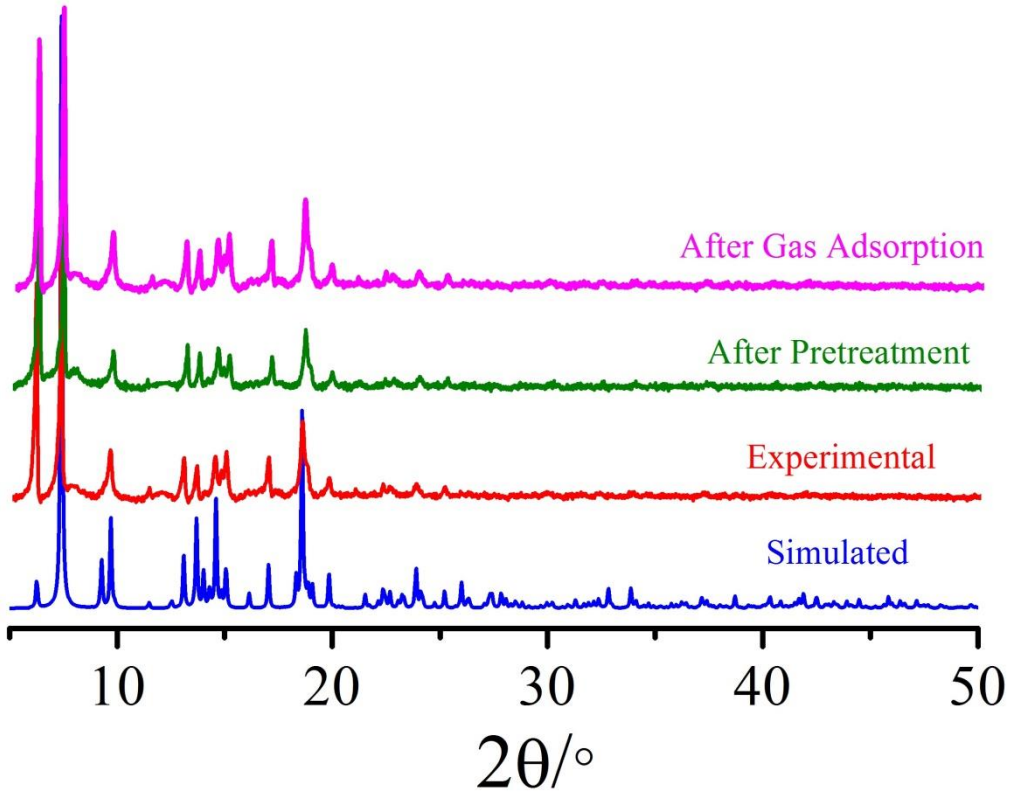

Fig. S28 PXRD pattern of MOF **4**.

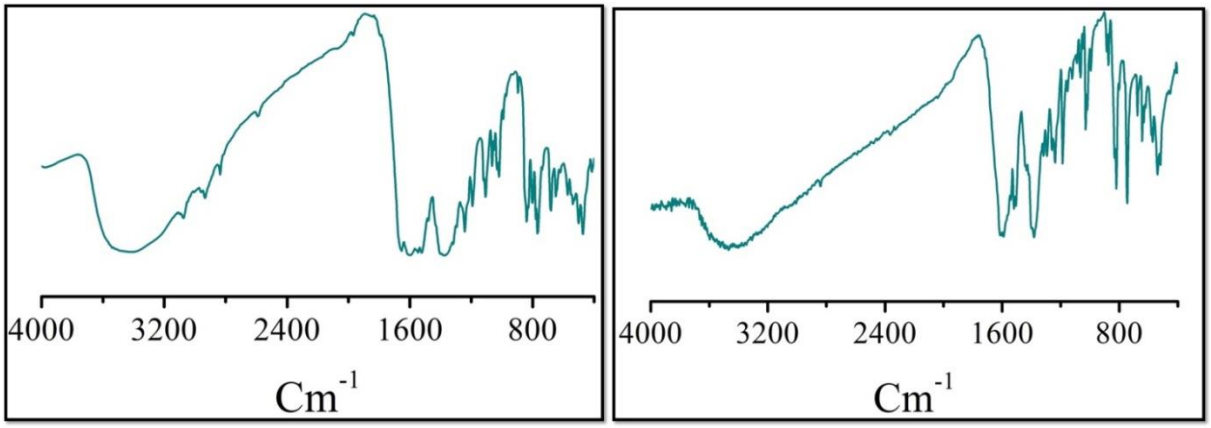

Fig. S29 IR spectrum of MOF **1** (left) and MOF **2** (right).

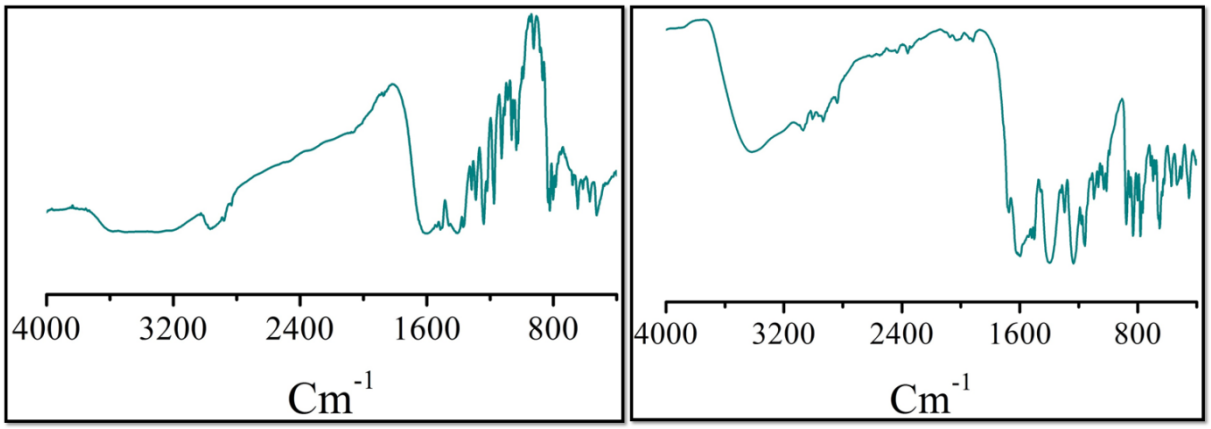

Fig. S30 IR spectrum of MOF **3** (left) and MOF **4** (right).